Catal Lett (2008) 124:204–214
DOI 10.1007/s10562-008-9465-x

A Simple and Efficient Route to Active and Dispersed Silica Supported Palladium Nanoparticles

Alexandra Barau · Vitaly Budarin · Agneta Caragheorgheopol · Rafael Luque · Duncan J. Macquarrie · Ambra Prelle · Valentin S. Teodorescu · Maria Zaharescu

Received: 14 December 2007 / Accepted: 13 March 2008 / Published online: 12 April 2008

Abstract Various mesoporous silica supported Pd materials were prepared by different methodologies in order to control and optimize the metal nanoparticle sizes for catalytic applications. The catalytic activities (conversion, mol% and selectivity to methyl-cinnamate) of the supported palladium catalysts were investigated in the Heck reaction under microwave irradiation using various haloarenes. Pd materials prepared by co-precipitation exhibited a very poor activity in the Heck reaction compared to that of Pd impregnated samples. Impregnated materials prepared without the use of a specific reducing agent had comparable activities to those of APTS-$NaBH_4$ reduced Pd materials, validating the simplicity of the methodology. High selectivities to methylcinnamate were obtained for all materials.

Keywords Mesoporous silica · Pd nanoparticles · Heterogenous catalysis · Heck reaction

A. Barau · A. Caragheorgheopol · M. Zaharescu
Institute of Physical Chemistry "Ilie Murgulescu" – Roumanian Academy, 202 Splaiul Independentei, 060021 Bucharest, Romania

V. Budarin · R. Luque (✉) · D. J. Macquarrie · A. Prelle
Green Chemistry Centre of Excellence, The University of York, Heslington, York YO10 5DD, UK
e-mail: rla3@york.ac.uk

V. S. Teodorescu
National Institute of Material Physics, 105bis Atomistilor, P.O. Box MG-7, 077125 Bucharest-Magurele, Romania

1 Introduction

Palladium nanoparticles, highly dispersed on various supports, have been widely studied over the last few years due to their interesting properties with applications as sensors, catalysts and in non-linear optics [1–8]. The properties and catalytic activities of the systems are highly dependent on the supports, methods of preparation, particle size, type and method of preparation of the noble metal. The type of support employed is indeed a critical factor in the performance of the resulting supported material [6, 7, 9, 10]. Two key features should be considered when employing a material as a support. Firstly, the material needs to be both thermally and chemically stable during the reaction process and secondly, the structure of the support has to be such that the active sites are well dispersed on its surface and that these sites are easily accessible. Generally, high surface areas (>100 $m^2\ g^{-1}$) and a mesoporous structure (pore size > 2 nm) meet the requirements for most applications. Mesoporous silicas, featuring a unique porous distribution, ease of tuneability and availability, appear to be one of the best candidates as support material for palladium nanoparticles based catalysts [10–14]. They offer high thermal and chemical stability and generally have high surface areas (>600 $m^2\ g^{-1}$) and pore sizes within the 1-20 nm range. Several methods of preparation of porous silicas have already been reported [10–16].

Different aspects should also be taken into consideration in the nanoparticles preparation, typically the incorporation of the palladium in the silica material as well as the maximum effective loading for the materials [3, 17, 18]. The presence of some functional groups on the support surface also plays a very important role in the phenomenon of particle agglomeration [19–21] as well as in the catalytic efficiency of the materials [20–26]. Furthermore, the

conventional preparation of metal nanoparticles involves the use of reducing agents including $NaBH_4$, hydrazine and molecular hydrogen which are not necessarily needed in many cases [8]. Most of the protocols reported are far away from being simple and environmentally friendly, involving several washing/conditioning steps to remove the excess of reducing agent. A simple and straightforward method for the preparation of palladium nanoparticles on different supports without the use of a specific reducing agent will be most advantageous.

The high surface area-to-volume ratio of noble metal nanoparticles makes them highly attractive tools for catalysis. The catalytic activity of such dispersed nanoparticles has been extensively studied over the last decade in various chemical reactions including oxidations, hydrogenations and hydrochlorinations [27–29].

Moreover, palladium is probably the most versatile metal in promoting or catalysing reactions, particularly those involving C–C bond formation, many of which are not easily achieved with other transition metal catalysts [30]. The Heck–Mizoroki coupling (Scheme 1) is an example of a C–C bond formation reaction that can be carried out using palladium supported catalysts [31]. It predates the Suzuki methodology and is one of the most useful derivations of palladium chemistry, giving us access to new extended alkenes via the addition of halides and triflates to alkenes [6, 22, 32, 33]. Although a few authors have reported reusable Pd materials for the Heck reaction [6, 7, 22], heterogeneous supported catalysts suffer from low turnover numbers (TON) and poor reusability [7, 30, 33] due to either aggregation of the palladium particles or leaching from the supports, providing soluble Pd species that give rise to the catalytic cycle in solution [34, 35]. Several studies attempting to address such important issue have been carried out, but there has been much scientific argument regarding the true catalytic species involved in the mechanism of cluster catalysis in the liquid phase that include low coordination sites [36, 37], active Pd atoms or ions leached in solution [38, 39] and Pd^{II} leached species in solution that catalyse the coupling reaction and then re-form the cluster [33, 40].

Herein, we report the facile preparation of highly active and stable silica supported palladium materials and their applications in C–C coupling reactions. The comparison between two different methods of preparation, with and without the use of reducing agent, is presented. We prove that the preparation of highly active and reusable nanoparticles supported on silica can be done without the need for additional reductant. The two different approaches made for the incorporation of the Pd onto the materials included co-gelation and post-synthesis wetness impregnation of the palladium precursor (in silica or in APTS-functionalized silica). $Pd(OAc)_2$ and ethanol (solvent) and $NaBH_4$ were used as Pd source and reducing agents, respectively. Materials with two Pd loadings (0.5 and 1 wt.%) were prepared.

2 Experimental

The porous SiO_2 matrix was prepared in the dodecylamine/acetonitrile/water system as previously reported [11]. The reagents employed including tetraethoxysilane (TEOS), 3-aminopropyl trimethoxysilane (APTS), acetonitrile, $Pd(COOCH_3)_2$, $NaBH_4$ (Aldrich) and *n*-dodecylamine (Fisher) were used as purchased without further purification. Ethanol was obtained from Fisher (HPLC grade) and deionised water was used in all preparations.

2.1 Preparation of the Silica Parent Material

Tetraethoxysilane (TEOS) was added dropwise to a stirred solution of *n*-dodecylamine in a water:acetonitrile (1:1 ratio) solution. The molar ratio employed was: 0.1 TEOS:0.03 *n*-dodecylamine:1.25 CH_3CN:2.8 H_2O. The mixture was stirred for 20 h at room temperature and a white solid was obtained. The final solid was filtered off, dried 24 h at 100 °C and subsequently extracted with ethanol in an automatic extractor to remove the template.

2.2 Preparation of Pd Nanoparticles on Silica

Three types of Pd containing materials were synthesized at two different Pd concentrations (0.5 and 1 wt.%). "In situ" materials were prepared by adding the corresponding quantity of $Pd(OAc)_2$ (Aldrich) into 5 mL EtOH, for the desired Pd loadings of 0.5 wt.% Pd (0.032 g Pd acetate) and 1 wt.% (0.064 g Pd acetate), into the solution of *n*-dodecylamine in a water:acetonitrile mixture (1:1 ratio), before the addition of TEOS. The synthesis was carried out in a similar way to that of the silica parent material.

The second type of materials were obtained after wetness impregnation of the SiO_2 matrix with an ethanol solution of $Pd(OAc)_2$ as follows: 0.005 and 0.01 g of Pd acetate (for 0.5 and 1 wt.% Pd loading, respectively) were dissolved in 5 mL EtOH and then added dropwise to a solution containing 1 g of the mesoporous silica dispersed in 100 mL EtOH. The final mixture was stirred for 24 h and the ethanol acts as direct reducing agent (together with the silanol groups on the silica surface) of the palladium as we have previously reported [8].

For the third type of materials, an additional functionalisation step was performed in order to functionalise the silica with aminopropyl groups. The parent silica was heated under reflux conditions in an ethanol solution of 3-aminopropyl trimethoxysilane (APTS) (3 mmol ATPS/1 g SiO_2) for 24 h. Pd was subsequently incorporated after wetness

impregnation of the functionalized silica with a acetone solution (5 mL) of $Pd(OAc)_2$ (0.005 and 0.1 g Pd acetate for the 0.5 and 1 wt.% Pd loadings) for 24 h. $NaBH_4$ (0.012 g) was employed as reducing agent.

The materials were filtered off from the reaction mixture and the resulting solutions were investigated by UV–Vis spectroscopy to identify the unreacted Pd precursor traces. The Pd content of the supported materials was also determined by ICP and elemental analysis after extracting the Pd from the sample using a HNO_3 diluted 2 M solution. In all cases, the different Pd deposition was carried out at room temperature.

2.3 Materials Characterisation

Nitrogen adsorption measurements were carried out at 77 K using an ASAP 2010 volumetric adsorption analyzer from Micromeritics. The samples were outgassed or 2 h at 100 °C under vacuum ($p < 10^{-2}$ Pa) and subsequently analyzed. The linear part of the BET equation (relative pressure between 0.05 and 0.22) was used for the determination of the specific surface area. The pore size distribution was calculated from the adsorption branch of the N_2 physisorption isotherms and the Barret-Joyner–Halenda (BJH) formula. The cumulative mesopore volume V_{BJH} was obtained from the PSD curve.

Conventional transmission electron microscopy (TEM) images were recorded on a JEOL 200CX electron microscope. High Resolution Transmission Electron Microscopy (HRTEM) images were recorded on a TOPCON 002B instrument.

Powder X-ray diffraction patterns (XRD) were recorded on a Bruker AXS diffractometer with CuKα ($\lambda = 1.5418$ Å), over a 2θ range from 5 to 85°, using a step size of 0.1° and a counting time per step of 4 s. To enable particle size analysis, the XRD patterns were recorder over the 5–85° range using a step size of 0.02° and a counting time per step of 20 s. Crystallite sizes were estimated by applying the Scherrer equation to the XRD line-widths of the different reflections [41, 42].

Diffuse reflectance infrared Fourier transform (DRIFT) spectra were recorded on a Brüker EQUINOX-55 instrument equipped with a liquid N_2 cooled MCT detector. Resolution was 2 cm^{-1} and 1024 scans were averaged to obtain the spectra in the 4000-600 cm^{-1} range. Spectra were recorded using KBr as reference. The samples for DRIFTS studies were prepared by mechanically grinding all reactants to a fine powder (sample/KBr 1/1000 ratio).

Thermogravimetric and thermodifferential analysis were performed using a Mettler Toledo TGA/SDTA851[e] and DSC823[e] equipment at a heating rates of 10 °C min^{-1}, under air, with typically 20 mg sample.

Temperature programmed reduction (TPR) was conducted on a Stanton-Redcroft STA750 thermal analyser under a 10 vol.% H_2/He stream with a total flow rate of 20 mL min^{-1} and ramp rate of 12 K min^{-1} between room temperature and 800 °C.

Microwave experiments were carried out in a CEM-DISCOVER model with PC control and monitored by sampling aliquots of reaction mixture that were subsequently analysed by GC/GC-MS using an Agilent 6890N GC model equipped with a 7683B series autosampler fitted with a DB-5 capillary column and an FID detector. Experiments were conducted on a closed vessel (pressure controlled) under continuous stirring. The microwave method was generally power controlled. The samples were irradiated with the maximum power output (300 W). Reaction products were also identified and confirmed by ^1H NMR using a JEOL 400 spectrometer operating at 400.13 MHz. Chemical shifts were calibrated using the internal $SiMe_4$ resonance.

A typical catalytic test was performed as follows: 0.5 mmol iodobenzene (0.83 mL), 0.5 mmol methyl acrylate (0.68 mL), 1 mL triethylamine and 0.1 g of catalyst were microwaved at 300 W (100 °C) for 5 min. Products were analyzed by GC using an Agilent 6890N GC model equipped with a 7683B series auto sampler. Only one main reaction product (methyl cinnamate) was obtained. The response factor of the main reaction product was determined with respect to the starting materials from GC analysis using known compounds in calibration mixtures of specified compositions.

The composition and preparation details for the Pd-silica materials are presented in Table 1.

Table 1 Summary of materials compositions and experimental details

Sample	Material	Pd incorporation method	Solvent	Pd reducing agent	Pd loading (%, ICP)
S1	SiO_2 + 0.5 wt.% Pd	In situ	EtOH	Ethanol	0.35
S2	SiO_2 + 1 wt.% Pd	In situ	EtOH	Ethanol	0.90
S3	SiO_2 + 0.5 wt.% Pd	Impregnation	EtOH	Ethanol	0.40
S4	SiO_2 + 1 wt.% Pd	Impregnation	EtOH	Ethanol	0.95
S5	SiO_2APTS(graft) + 0.5 wt.% Pd	Impregnation	Acetone	$NaBH_4$	0.55
S6	SiO_2APTS(graft) + 1 wt.% Pd	Impregnation	Acetone	$NaBH_4$	0.95

3 Results and Discussion

3.1 Pd Loading and Textural Properties

Mesoporous silica supported Pd materials were obtained in all three experimental conditions presented above. The UV–Vis spectra of the resulting solutions after the materials were filtered off from the reaction bath suggested that some traces of unreacted palladium acetate were present only when ethanol was chosen as Pd reducing agent, confirming the deposition of the Pd in the silica matrix. TPR experiments (not shown, only a flat line was found) confirmed that only reduced platinum was present in all samples (no reduction peaks due to Pd^{2+} were found in any of them), irrespective of the metal loading in the material.

The Pd content of the investigated samples was determined using elemental analysis and ICP and included in Table 1. The Pd loadings were in good agreement with the UV–Vis results showing the most of the Pd was incorporated into the final solid.

The mesoporous character of the obtained materials was confirmed both by porosity measurements and TEM.

The materials exhibited the typical type IV adsorption–desorption isotherms, characteristics of mesoporous materials. The textural properties of the various silica materials are summarized in Table 2.

The Pd-silica materials exhibited lower surface areas compared to the parent material. This effect was especially noticeable when increasing the Pd loading in samples (S4 and S6). Pore volumes remained unchanged between Pd samples, although they were considerably reduced after the palladium incorporation compared to those of the parent silica (from 0.7 to 0.5–0.35 $cm^3\ g^{-1}$). The surface area of the materials also decreased with increasing the Pd loading in samples as expected (Table 2). Pd materials showed a very homogeneous pore distribution that was affected by the palladium loading in the samples. Thus, an increase in Pd loading from 0.5 to 1 wt.% decreased the pore diameter from 3 to 2 nm, suggesting that the palladium may be deposited within the matrix pores. These results were in good agreement with the results of the average nanoparticle size obtained from TEM and XRD (Table 2).

3.2 Transmission Electron Microscopy (TEM) Experiments

The silica parent material has a large surface area being mostly mesoporous. The flower like shape morphology of the SiO_2 matrix was revealed by tilting the specimen in the microscope. Some projections of this morphology show an intermediate porosity "lake" of about 20–40 nm wide and 200 nm deep is formed between the "flower petals", allowing an easy access inside the silica aggregate matrix volume at the real nanometric pores of the silica structure. At this magnification, the Pd nanoparticles cannot be resolved.

Representative TEM micrographs of the silica supported palladium materials have also been included in Fig. 1. The TEM of the S4 sample at higher magnification clearly shows Pd nanoparticles with particle sizes ranging from 2 to 5 nm. The particle sizes were found to vary depending on the methodology employed in the reduction.

Thus, the materials prepared using EtOH as both solvent and reducing agent have bigger nanoparticles (e.g. average size 3.9 nm S3) compared to those of the $NaBH_4$ reduced samples (e.g. average size 2.5 nm S6). They also show a tendency to aggregate on the surface of the mesoporous silica at higher loadings and the nanoparticles were less homogeneously dispersed. HRTEM micrographs showed that particles bigger than 7-8 nm are in fact Pd nanoparticle aggregates (Fig. 2, corner). The HRTEM images also revealed the presence of some bigger particle aggregates on S4 sample.

3.3 Powder X-Ray Diffraction (XRD) Measurements

Powder XRD diffraction patterns (Fig. 3) obtained for the mesoporous materials exhibited a broad reflection

Table 2 Textural properties (surface area, S_{BET}; Pore diameter, D_{BJH} and pore volume, V_{BJH}) and average nanoparticle sizes estimated by TEM (averaging 50 nanoparticles) and XRD (using the Scherrer equation) of the different silica supported palladium samples

Material	Method of preparation	S_{BET} ($m^2\ g^{-1}$)	D_{BJH} (nm)	V_{BJH} (mL g^{-1})	Average particle size by XRD (nm)	Average particle size by TEM (nm)
Silica	Silica parent material	821	3.1	0.55	–	–
S1	In situ	676	2.4	0.54	5.6	5.7
S2	In situ	494	2.3	0.40	5.1	5.1
S3	Impregnation	807	2.4	0.57	3.6	3.9
S4	Impregnation	383	2.5	0.32	4.0	4.1
S5	Funct(APTS) + impreg	540	2.1	0.36	3.2	3.3
S6	Funct(APTS) + impreg	420	2.0	0.32	2.5	2.5

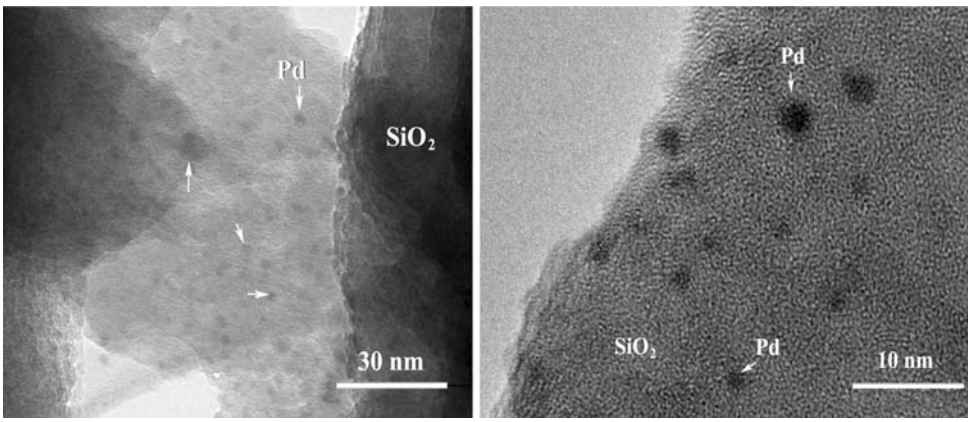

Fig. 1 TEM images (different magnifications) of S4 sample, showing the Pd nanoparticles (*arrows*) on the silica support

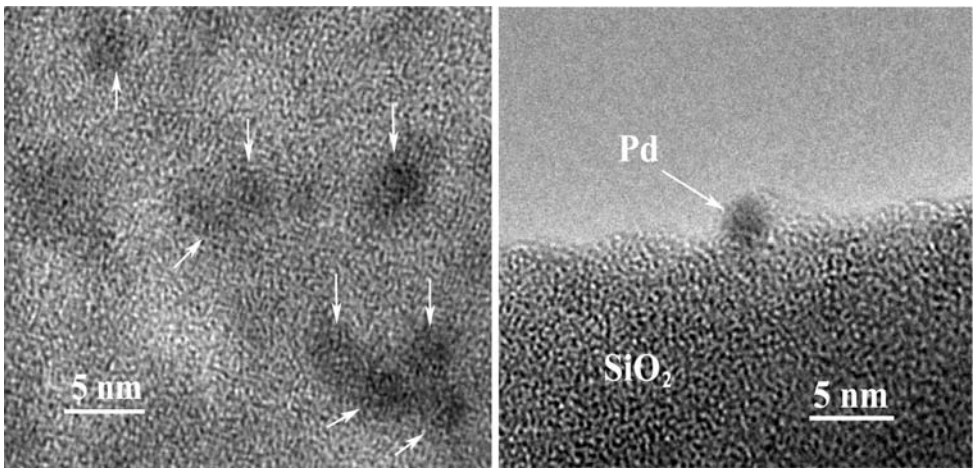

Fig. 2 HRTEM images of material S6. Pd nanoparticles on the silica support (*right*) and on the edges of the silica support (*left*)

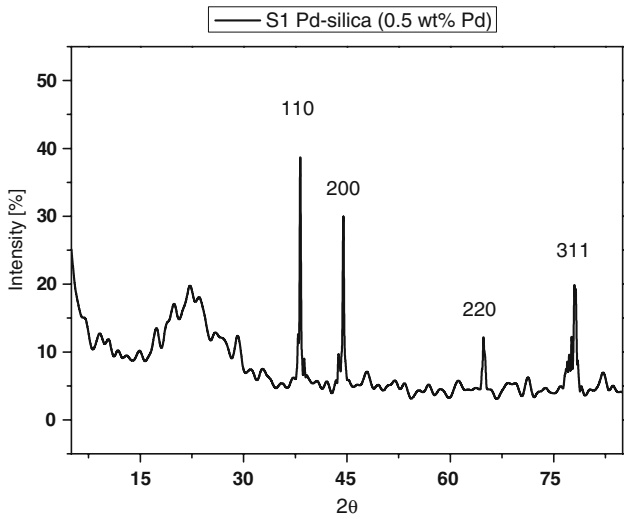

Fig. 3 XRD diffraction patterns of the S1 silica supported palladium material (0.5 wt.% Pd)

corresponding to the amorphous silica support. Four additional reflections were found in the XRD pattern that could be attributed to elemental palladium, in good agreement with the JCPDS 46-1043 file [42]. All materials prepared exhibited a similar XRD pattern. Of note was the absence of any other reflections in the diffractogram, indicating the absence of significant quantities of the Pd precursor on the support. The Pd nanoparticle size was estimated from the XRD pattern using the Scherrer equation [41]. The average nanoparticle sizes (Table 2) were found to be in good agreement with the TEM results.

3.4 Diffuse Reflectance Infrared Spectroscopy (DRIFT) Measurements

DRIFT spectra of the silica supported palladium nanoparticles compared to the silica parent material were recorded (Fig. 4). No traces of Pd precursor or PdO were detected by IR spectroscopy which suggests that metallic Pd may be present in the materials, in good agreement with the Pd loadings of the materials, EDX, TPR and TEM results. The DRIFT spectra showed the typical vibration modes from silica, namely: ν_{as} Si–O–Si at 1115 and 1090 cm^{-1}, ν Si–O(H) at 975 cm^{-1}, ν_s Si–O–Si at 800 cm^{-1} and δ Si–O–Si at 470 cm^{-1}, as reported by Bertoluzza [43]. In addition, the corresponding vibrations due to the presence of organics in

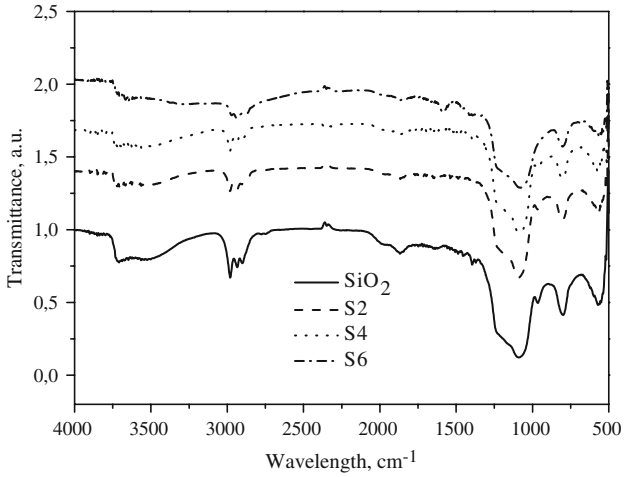

Fig. 4 DRIFT spectra of the mesoporous parent silica compared to all 1 wt.% Pd samples (S2, S4 and S6) prepared by different routes

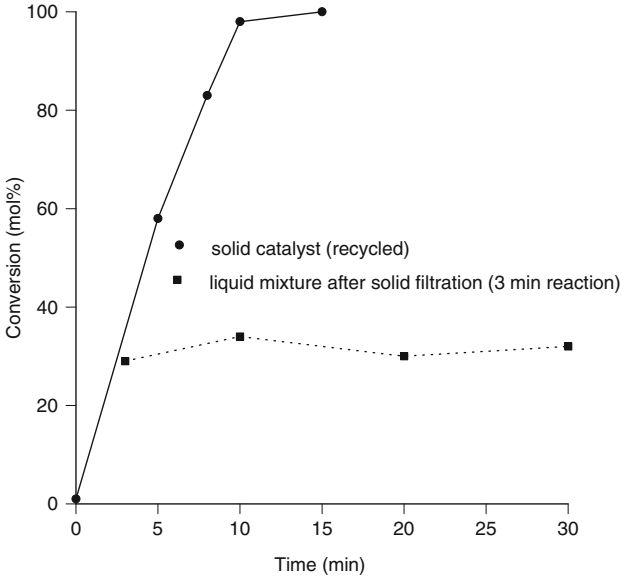

Fig. 5 Hot filtration test profile (performed after 3 min) of material S6 in the Heck reaction using iodobenzene as starting material. *Solid line*: reused S6 material performance in the Heck reaction; *discontinuous line*: liquid mixture filtered off after reaction (3 min, conversion 30%) and further reacted for 30 min

the composition of the studied samples, as methyl (ν_{as} CH_3 at 2980 cm^{-1}, ν_s CH_3 at 2820 cm^{-1}) or ethyl groups (ν_{as} CH_3 at 2980 cm^{-1}, ν_{as} CH_2 at 2860 cm^{-1} ν_s CH_3 2830 cm^{-1}) could be identified. The presence of the organic residue in the studied material could be correlated to the incomplete extraction of the templating agent after the extraction process.

3.5 Thermogravimetric and Thermodifferential Analysis (TG/DTA)

The results of the thermogravimetric and thermodifferential analysis of the samples are summarized in Table 3.

The decomposition of the samples takes place stepwise irrespective of the preparation route. The physisorbed water was removed at low temperatures (<100 °C) and the evolution of the structural OH and the burning out of the organic traces take place at temperatures ranging between 200 and 600 °C (13% mass loss, exotherm peak). The peak at 837 °C can be attributed to the water loss due to dehydroxylation of SiOH groups. Results were in good agreement with the DRIFT measurements that indicated the presence of some organic traces in the samples.

3.6 Catalytic Activity: The Heck Coupling

The materials were then tested for their catalytic activity in the Heck reaction under microwave conditions. Various haloarenes (iodo- bromo- and chlorobenzene) and methylacrylate were employed as substrate (Scheme 1). Methyl cinnamate was the main product obtained in the reaction. Results are summarized in Tables 4–7.

Table 3 DTA/TGA peak assignments of various silica supported palladium materials

Sample	Temp. range (°C)	Peak position (°C)		Total weight loss (%)	Attribution
		Exo	Endo		
S2	20–200		39,95	13	Removal of physisorbed water and R-OH evolution
	200–400		234		Templating agent decomposition
	400–1000		548		Templating agent traces decomposition
S4	20–200		61	15	Removal of physisorbed water and R-OH evolution
	200–400		285		Templating agent decomposition
	400–1000	537	837		Removal of templating agent traces and dehydroxylation of Si-OH groups
S5	20–200		66	11	Removal of physisorbed water and R-OH evolution
	200–400	298			Removal of templating agent traces
	400–1000		937		Si-OH dehydroxylation

Interestingly, the materials exhibited catalytic activities depending not only on the palladium content but also depending on the method of the palladium incorporation into the silica material. The silica parent material was not active in the Heck reaction as expected but the palladium supported materials prepared by impregnation showed better catalytic activities compared to the in situ materials (Table 4). The Pd loading in the samples was slightly different in the 0.5% loadings and this obviously had an influence in the improved catalytic activity of the impregnated solids compared to the in situ prepared materials. The nanoparticle size seemed to have a critical effect on the catalytic activity of the materials. The catalysts with smaller nanoparticle sizes were found to be more active in the coupling reaction (Table 4).

APTS functionalised palladium catalysts obtained after impregnation provided improved activities compared to the impregnated materials implying a stabilisation of the nanoparticles in the samples, in good agreement with previous reports [20, 22]. Materials with higher palladium loading (1 wt.%) also performed better than those with lower palladium (0.5 wt.%). Quantitative conversion to methyl cinnamate was obtained for both impregnated materials (APTS functionalised and non-functionalised) after 10 min of reaction under microwave irradiation using iodobenzene as substrate. Results have been only included in a separate table (Table 6, optimised data) as materials S3 to S6 provided similar results (90–98% conversion and >95% selectivity to methyl-cinnamate) so that a comparison in terms of catalyst efficiency was not possible in these conditions. The in situ palladium material S2 gave a relatively poor 65% conversion under the same reaction conditions. In any case, the materials were highly selective to methyl cinnamate, the only product obtained in the Heck reaction.

X = Br, Cl, I

Scheme 1 Heck reaction scheme

Preliminary experiments showed the S6 material was the most active catalyst in the Heck reaction (APTS functionalised + higher palladium content), providing a 56% conversion (>99% selectivity) after 5 min of reaction under microwave irradiation, a similar conversion to that obtained with our previously reported highly active palladium nanoparticles on polysaccharide derived mesoporous materials [8]. Active APTS functionalised zeolite materials in the Heck reaction have also been reported [22]. A conversion of 98% (>95% selectivity) was obtained after 10 min under the same conditions. Compared to S6, the homogeneous reaction (employing similar Pd quantities of palladium acetate to the Pd silica loadings found in our materials) provided a poor 21% conversion of starting material compared to that of S6 (Table 4, entry 7). We then decided to investigate the effect of the reaction time, temperature and quantity of catalyst employed in the conversion and selectivity to methyl cinnamate for our palladium systems. Results are summarised in Table 5. Albeit all parameters were found out to have an influence on the catalytic activity of the palladium systems, the time of microwave irradiation was particularly effective in terms of improving the conversion of the systems in the Heck reaction. Shorter reaction times than 3–4 min provided conversion values lower than 50%, but of note was the 25% conversion (>99% selectivity to methyl cinnamate) after 1 min, interestingly much higher to that obtained for the S2 material (1 wt.% palladium prepared in situ) after 5 min. A further increase in temperature from 5 to 10 min provided quantitative conversion to methyl cinnamate.

The effect of the temperature in the reaction was also studied. An increase in the catalyst efficiency was observed when increasing the temperature of reaction although this

Table 4 Catalytic activities [Conversion (mol%) and selectivity to methyl-cinnamate, $S_{\text{m-cinnamate}}$ (mol%)] of various catalysts including our silica supported palladium materials in the Heck reaction employing iodobenzene as substrate[a]

Catalyst	Method of preparation	Pd loading (wt.%)	Conversion (mol%)	$S_{\text{m-cinnamate}}$ (mol%)	Nanoparticle size (TEM/XRD)
$Pd(OAc)_2$[b]	–	–	21	>90	–
S1	In situ	0.5	<5	>99	5.6/5.7
S2	In situ	1.0	<20	>99	5.1/5.1
S3	Impregnation	0.5	35	>99	3.6/3.9
S4	Impregnation	1.0	40	>99	4.0/4.1
S5	Funct + impreg	0.5	40	>99	3.2/3.3
S6	Funct + impreg	1.0	56	>99	2.5/2.5

[a] Reaction conditions: 300 W, 5 min, 100 °C, 0.1 g catalyst

[b] 0.001 g $Pd(OAc)_2$ (equivalent to a loading of over 1 wt.% Pd on silica) was employed to run the homogeneous reaction

Table 5 Effect of the different parameters (time, temperature of reaction and quantity of catalyst) in the conversion (mol%) and selectivity to methyl-cinnamate ($S_{m\text{-cinnamate}}$) of the S6 material in the Heck reaction employing iodobenzene as substrate

Effect of the time of reaction (Conditions: 300 W, 0.1 g catalyst)					
Time (min)	1	3	5	8	10
Maximum temperature (°C)	101	106	107	110	116
Conversion (mol%)	25	43	56	85	98
$S_{m\text{-cinnamate}}$ (mol%)	>99	>99	>99	>99	>95
Effect of the temperature of reaction (Conditions: 300 W, 0.1 g catalyst, 5 min)					
Average temperature (°C)	80	100	130	150	180
Conversion (mol%)	40	56	69	75	88
$S_{m\text{-cinnamate}}$ (mol%)	>99	>99	>99	>99	>99
Quantity of catalyst (Conditions: 300 W, 5 min)					
Quantity of catalyst (g)	0.025	0.050	0.100	0.200	0.400
Maximum temperature (°C)	102	106	107	112	114
Conversion (mol%)	20	36	56	88	>99
$S_{m\text{-cinnamate}}$ (mol%)	>99	>99	>99	>99	>95

increase in catalytic activity was not as effective as an increase in the time of reaction. Another parameter investigated was the quantity of catalyst employed in the reaction. As expected, an increase in the quantity of catalyst increased the conversion in the systems (Table 5). Of particular interest was an almost doubled conversion when increasing the quantity of catalyst from 0.1 to 0.2 g. The selectivity of the samples was not significantly affected by either an alteration on the temperature or an increase in the quantity of catalyst. The effects observed were similar to all the catalysts screened in the reaction. A similar effect was found for all catalysts tested in the coupling reaction.

Finally, optimised results for the use of iodobenzene as starting material are summarised in Table 6. A quantitative conversion to methyl cinnamate in excellent selectivities could easily be achieved under microwave irradiation (300 W) for 10 min at low temperature (100 °C) for most of the prepared palladium supported materials. The silica supported palladium materials prepared by impregnation exhibited improved catalytic activities compared to the homogeneous system in which Pd acetate was employed as catalyst (Table 6, entry 1).

Interestingly, the materials prepared without the use of a specific reducing agent (EtOH, S3 and S4) exhibited almost comparable activities and selectivities in the reaction (only slightly lower), validating the appropriateness of the use of EtOH as reducing agent [8].

Compared to iodobenzene, the reaction runs using bromobenzene as substrate provided moderate to good conversions of the starting material with a very high selectivity to methyl cinnamate, although a longer time of reaction was needed to achieve such conversion values. Results are included in Table 7. Finally, poor results with chlorobenzene as starting material were obtained with all catalysts screened in the Heck reaction. Only a promising activity (35% conversion after 30 min reaction) was found for S6.

The activity of the nanoparticles can be correlated to the Pd(0) supported on silica. Thus, the difference in activity in the materials is believed to be due to the differences in the nanoparticle dispersion and the nanoparticle sizes. A

Table 6 Optimised catalytic activities [Conversion (mol%) and selectivity to methyl-cinnamate, $S_{m\text{-cinnamate}}$ (mol%)] of various palladium catalysts in the Heck reaction employing iodobenzene as substrate[a]

Catalyst	Method of preparation	Pd loading (wt.%)	Conversion (mol%)	$S_{m\text{-cinnamate}}$ (mol%)
$Pd(OAc)_2$[b]	–	–	69	>90
S1	In situ	0.5	<10	>99
S2	In situ	1.0	40	>99
S3	Impregnation	0.5	70	>95
S4	Impregnation	1.0	89	>90
S5	Funct + impreg	0.5	90	>95
S6	Funct + impreg	1.0	98	>95

[a] Reaction conditions: 300 W, 10 min, 100 °C, 0.1 g catalyst

[b] 0.001 g $Pd(OAc)_2$ (equivalent to a loading of over 1 wt.% Pd on silica) was employed to run the homogeneous reaction

Table 7 Optimised catalytic activities [Conversion (mol%) and selectivity to methyl-cinnamate, $S_{m\text{-}cinnamate}$ (mol%)] of various palladium catalysts in the Heck reaction employing bromobenzene as substrate[a]

Catalyst	Method of preparation	Pd loading (wt.%)	Conversion (mol%)	$S_{m\text{-}cinnamate}$ (mol%)
$Pd(OAc)_2$[b]	–	–	82	>90
S1	In situ	0.5	<10	>99
S2	In situ	1.0	31	>99
S3	Impregnation	0.5	55	>99
S4	Impregnation	1.0	72	>99
S5	Funct + impreg	0.5	84	>95
S6	Funct + impreg	1.0	>95	>90

[a] Reaction conditions: 300 W, 30 min, 90–110 °C, 0.1 g catalyst

[b] 0.001 g $Pd(OAc)_2$ (equivalent to a loading of over 1 wt.% Pd on silica) was employed to run the homogeneous reaction

decrease in the nanoparticle size increased the activity of the materials

A comparison of the activities and selectivities of our Pd-silica materials with various reported systems in the Heck reaction has been included in Table 8. The reported silica supported nanoparticles afforded excellent conversions and complete selectivities to methyl cinnamate in a short period of time under microwave irradiation. The microwave protocol was proved to be efficient and more environmentally friendly than many of the reported methodologies using Pd/or similar Pd/SiO_2 systems.

3.7 Leaching and Materials Reusability Investigations

A hot filtration test (HF) was performed to assess the truly heterogeneous nature of our catalytic reaction (Fig. 5). The catalyst was filtered off after 3 min of mw irradiation (around 30% conversion using iodobenzene as starting material). The reaction mixture without catalyst was then further microwaved for 30 additional minutes and finally quenched. No changes in conversion were observed (Fig. 5, discontinuous line), excluding the presence of any palladium leached species in solution.

Table 8 Comparison of catalytic activities of different palladium supported catalysts in the Heck reaction of iodobenzene with methyl acrylate

References	Reaction conditions	Catalyst	Conversion (mol%)	$S_{m\text{-}cinnamate}$ (mol%)
Our work	Microwaves, 300 W, 100-110 °C, 5 min	S4-Pd-SiO_2 1% Pd	72	>99
	0.5 mmol iodobenzene, 0.1 g catalyst	S6-Pd-SiO_2 1% Pd	>95	>90
[44]	Ultrasounds, RT, 10 h, 10 mmol iodobenzene, 0.2 g catalyst	Pd/C 10% Pd	71	>99
[40]	100 °C, 1 h, 2 mmol iodobenzene	Pd/C 10% Pd	92	>99
[45]	140 °C, 0.5 h, 5 mmol iodobenzene, 0.08 g catalyst	Pd/C 10% Pd	>99	>99
[45]	140 °C, 0.5 h, 5 mmol iodobenzene, 0.15 g catalyst	Pd/C 1% Pd	>99	>99
[46]	90 °C, 12 h, 2 mmol iodobenzene, 0.2 mol% catalyst	Pd-colloid	89	>99
[47]	85 °C, 12 h, 1 mmol iodobenzene, 0.05 g catalyst	Pd-cellulose 5% Pd	>99	>99
[48]	150 °C, 1 h, 1 mmol iodobenzene, 0.3 mol% catalyst	Pd-MCM-41 1.4% Pd	>99	>99
[49]	150 °C, 2 h, 0.89 mmol iodobenzene, 0.068 g catalyst	Pd-SiO_2 1.5% Pd	81	>99
[45]	140 °C, 0.5 h, 5 mmol iodobenzene, 0.15 g catalyst	Pd-SiO_2 1% Pd	>99	>99
[7]	Microwaves, 60 W, 10 min	Pd/KF-Al_2O_3	62	>99

Moreover, the materials were reused after reaction completion (Fig. 5, solid line). Solids were filtered off, washed thoroughly with acetone and methanol and dried overnight at 100 °C prior reutilization in the Heck reaction. The palladium supported materials were found to be reusable up to four times without an appreciable loss of activity (e.g. material S6 gave an 89% conversion, >95 selectivity to methyl cinnamate after four uses). Similar reusability behaviour was found for all the Pd catalysts screened in the test reaction. No significant quantities of Pd (less than 2 ppm) were found in solution after analysis of the final solution after the reaction, in good agreement with the hot filtration test results, confirming the high activity and stability of our silica supported Pd materials.

4 Conclusions

The preparation of silica supported palladium nanoparticles was successfully accomplished by all the three methods proposed (co-gelation, post-synthesis wetness impregnation of the palladium precursor in silica or in APTS-functionalized silica) and materials successfully employed in the Heck reaction under microwave conditions using various haloarenes.

Interesting differences in catalytic activity between materials were found. Pd materials prepared by co-gelation exhibited a rather poor activity in the Heck reaction compared to that of Pd impregnated samples. The APTS functionalisation plus $NaBH_4$ reduction in the palladium materials seemed to generate a homogeneously distributed nanoparticle system and stabilised the materials that were found to be the most active of all the catalysts screened in the Heck reaction. Nevertheless, the materials prepared using EtOH as both solvent and reducing agent were proved to be similarly active and selective in the Heck coupling, confirming the validity of the use of EtOH (together with silanol groups on the materials surface) as metal reductant. Selectivity was very good, as methyl cinnamate was the only product obtained in the coupling reaction, and the materials were found to be highly stable, active and reusable without appreciable loss of activity.

Acknowledgments This work was supported partially by projects CEEX 23/2006, CEEX III 2/2005 and CEEX 42/2005.

References

1. Chen CS, Chen HW (2004) Appl Catal A 260:207
2. Robles-Dutenhefner PA, Speziali MG, Sousa EMB, dos Santos EN, Gusevskaya EV (2005) Appl Catal A 295:52
3. Han YF, Kumar D, Sivadinarayana C, Goodman DW (2004) J Catal 224:60
4. Sasahara T, Kido A, Ishihara H, Sunayama T, Egashira M (2005) Sensor Actuators B 108:478
5. Ichinde T, Masaki S, Uchida K, Nozaki S, Morisaki H (2004) Thin Solid Films 466:27
6. Polshettiwar V, Molnar A (2007) Tetrahedron 63:6949
7. Yin L, Liebscher J (2007) Chem Rev 107:133
8. Budarin V, Clark JH, Luque R, Macquarrie DJ, White RJ (2007) Green Chem doi:10.1039/B715508E
9. Smith K (ed) (1992) Solid supports and catalysts in organic reactions. Ellis Horwood Ltd, Chichester
10. Taguchi A, Schüth F (2005) Micropor Mesopor Mater 77:1
11. Macquarrie DJ, Gilbert BC, Gilbey LJ, Caragheorgheopol A, Savonea F, Jackson DB, Onida B, Garrone E, Luque R (2005) J Mater Chem 15:3946
12. Yuranov I, Kiwi-Minsker L, Buffat P, Renken A (2004) Chem Mater 16:760
13. Corma A (1997) Chem Rev 97:2373
14. Huang L, Wang Z, Ang TP, Tan J, Wong PK (2006) Catal Lett 112:219
15. Shen S, Chen F, Chou PS, Pharavudkikul P, Zhu K, Tan RBH (2006) Micropor Mesopor Mater 92:300
16. Liu J, Yang Q, Zhao XS, Zhang L (2007) Micropor Mesopor Mater 106:62
17. Panpranot J, Phandinhong K, Proserthdam P, Hasegawa M, Fujita S, Arai M (2006) J Mol Catal A 253:20
18. Yang LM, Wang YJ, Sung YW, Luo GS, Dai YY (2006) J Colloid Interface Sci 299:823
19. Lewis LN (1993) Chem Rev 93:2693
20. Underhill RS, Liu GJ (2000) Chem Mater 12:3633
21. Alvarez J, Liu J, Roman E, Kaifer AE (2000) Chem Commun 1151
22. Mandal S, Roy D, Chaudhari RV, Sastry M (2004) Chem Mater 16:3714
23. Yang Y, Liu J, Yang J, Kapoor HP, Inagaki S, Li C (2004) J Catal 228:265
24. Li M, Seshan K, Lefferts L (2004) Appl Catal B 50:143
25. Besson E, Mehdi A, Matsutra V, Guari Y, Reye C, Corriu JP (2005) Chem Commun 1775
26. Cheng W, Zhou Z, Miao W, Chen H, Huang B, Tang T (2006) Mater Lett 60:1843
27. Karimi B, Zamani A, Clark JH (2005) Organometallics 24:4695
28. Karimi B, Abedi S, Clark JH, Budarin V (2006) Angew Chem Int Ed 45:4776
29. Karimi B, Biglari A, Clark JH, Budarin V (2007) Angew Chem Int Ed 46:1
30. Tsuji J (2004) Palladium reagents and catalysts. Wiley-VCH
31. Heck RF, Nolly JP (1972) J Org Chem 37:2320
32. Al-Hashimi M, Sullivan AC, Wilson JRH (2007) J Mol Catal A 273:298
33. Biffis A, Zecca M, Basato M (2001) J Mol Catal A 173:249
34. Mehnert P, Weaver DW, Ying JY (1998) J Am Chem Soc 120:12289
35. Wagner M, Kohler K, Djakovitch L, Weinkauf S, Hagen V, Muhler M (2000) Top Catal 13:319
36. Bradley J, Tesche B, Busser W, Maase M, Reetz MT (2000) J Am Chem Soc 122:4631
37. Narayanan R, El-Sayed MA (2003) J Am Chem Soc 125:8340
38. Reetz MT, Westermann E (2000) Angew Chem Int Ed 39:165
39. Gaikwad AV, Holuigue A, Thathagar MB, ten Elshof JE, Rothemberg G (2007) Chem Eur J 13:6908
40. Biffis A, Zecca M, Basato M (2001) Eur J Inorg Chem 1131
41. Kulg H, Alexander L (1974) X-ray diffraction procedures. Wiley, New York
42. Palladium JCPDS (1969) 46-1043
43. Bertoluzza A, Fagnano C, Moreli MA, Gottaradi V, Guglielmi M (1982) J Non Cryst Solids 48:117

44. Ambulgekar GV, Bhanage BM, Samant SD (2005) Tetrahedron Lett 46:2483
45. Zhao F, Bhanage BM, Shirai M, Arai M (2000) Chem Eur J 6:843
46. Zheng P, Zhang W (2007) J Catal 250:324
47. Reddy KR, Kumar NS, Reddy PS, Sreedhar B, Kantam ML (2006) J Mol Catal A 252:12
48. Papp A, Galbacs G, Molnar A (2005) Tetrahedron Lett 46:7725
49. Molnar A, Papp A, Mirlos K, Forgo P (2003) Chem Commun 2626